Research on Design of Asynchronous Motor Flux Observer Considering Iron Loss

Yaoheng Li[1], Jiangtao Gai[1], Guangming Zhou[1] and Zhengda Han[1]

[1]Science and Technology on Vehicle Transmission Laboratory, China North Vehicle Research Institute, Beijing 100072, China

E-mail:yaohengli201@qq.com

Abstract: With the increasing importance of energy conservation emission reduction, the research about how to improve the operating efficiency of asynchronous motor has become a hot topic in the field of high-performance transmission. Among many efficiency optimization algorithms, the control method based on loss model (LMC) is widely concerned because of its clear physical meaning and fast optimization speed. The core of LMC is to ensure that the instruction of optimized flux can be accurately controlled which can realize the complete decoupling of the torque and flux in the FOC. Based on the model of asynchronous motor considering iron loss, the paper deduces the flux expression of asynchronous motor and proposes an improved flux observer. Finally, the feasibility and effectiveness of the proposed control strategy are verified by simulation and experiment.

1. Introduction

Asynchronous motor has been widely used in the field of transmission for its advantages of simple structure, high reliability and low maintenance cost [1]. Asynchronous motor can achieve high efficiency near rated load. However, its application is limited by its low efficiency in light load condition. With the increasing importance of energy conservation emission reduction, the research about how to improve the operating efficiency of asynchronous motor has become a hot topic in the field of high-performance transmission.

The research on the optimal control of asynchronous motor efficiency has been for nearly 40 years. Among many efficiency optimization algorithms, the control method based on loss model (LMC) is widely concerned because of its clear physical meaning and fast optimization speed [2]. The core of LMC is to ensure that the instruction of optimized flux can be accurately controlled which can realize the complete decoupling of the torque and flux in the FOC. According to the basic concept, the accuracy of flux observer based on the voltage model is greatly affected by stator current and other parameters. In the actual operation of the motor, the sensor error, electromagnetic interference, sampling error and other problems often lead to DC bias error in current sampling. In the integration process, small DC bias will lead to integral saturation, which will become more significant if no improvement measures are taken. In terms of the current research situation, scholars tend to ignore the existence of iron consumption. However, the iron consumption of induction motor is actual existence. In addition, scholars usually use a first-order low-pass filter instead of a pure integral link to eliminate the cumulative influence of dc bias, but the low-pass filter will produce amplitude and phase errors of flux observation. Especially at low speed, the error of stator current sensor detection will be more serious due to the large stator resistance pressure drop [3-5].

This article obtains from the loss of induction motor model, and sets up the flux observer expression considering iron loss of voltage model. Furthermore, the paper optimizes the flux observer based on the voltage model and adjusts the cut-off frequency of filter online. What's more, by the real-time compensation caused by amplitude and phase error, the flux observer is within the scope of the motor at full speed all have ideal effect, and improves the system performance. Finally, the theory of this paper is verified by simulation and experiment.

2. Research on improved flux observer of voltage model considering iron

The control core of the optimal control strategy of asynchronous motor based on loss model is to control the flux of asynchronous motor with optimal flux instruction. In order to consider the actual running condition of the actual motor, it is necessary to deduce the flux observer of voltage model considering iron.

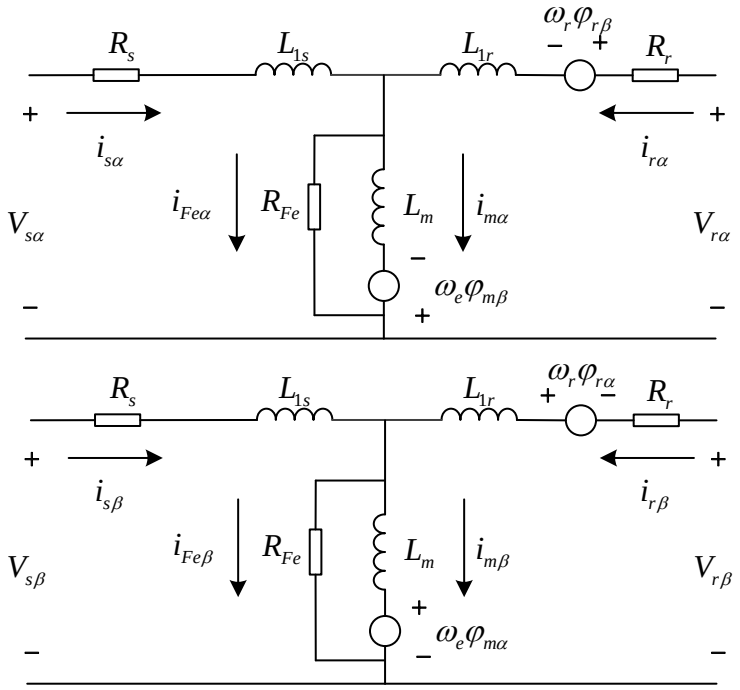

Figure 1. Mathematical parallel model under static coordinates considering iron loss of motor

In Figure1, $i_{s\alpha}$ and $i_{s\beta}$ are the current of stator α、β axis. $I_{r\alpha}$ and $i_{r\beta}$ are the current of rotor α、β axis . $V_{s\alpha}$ and $V_{s\beta}$ are the voltage of stator α、β axis. $\varphi_{m\alpha}$ and $\varphi_{m\beta}$ are the main flux of α、β axis. $I_{Fe\alpha}$ and $i_{Fe\beta}$ are the iron consumption equivalent winding current of α、β axis. According to the equivalent circuit diagram in Figure 1. The flux observer expression can be deduced as follow:

$$\begin{cases} V_{s\alpha} = R_s i_{s\alpha} + \dfrac{d\varphi_{s\alpha}}{dt} \\ \varphi_{s\alpha} = L_m i_{s\alpha} + L_r i_{r\alpha} - L_m i_{Fe\alpha} \\ \varphi_{r\alpha} = L_m i_{s\alpha} + L_r i_{r\alpha} - L_m i_{Fe\alpha} \end{cases} \tag{1}$$

$$\begin{cases} \varphi_{s\alpha} = \int (V_{s\alpha} - R_s i_{s\alpha}) dt \\ \varphi_{r\alpha} = \dfrac{L_r}{L_m}(\varphi_{s\alpha} - L_\sigma i_{s\alpha}) + L_{lr} i_{Fe\alpha} \end{cases} \tag{2}$$

In a similar way:

$$\begin{cases} \varphi_{s\beta} = \int (V_{s\beta} - R_s i_{s\beta}) dt \\ \varphi_{r\beta} = \dfrac{L_r}{L_m} (\varphi_{s\beta} - L_\sigma i_{s\beta}) + L_{lr} i_{Fe\beta} \end{cases} \tag{3}$$

It can be seen from the above equation that the integral link plays a crucial role in the relation of magnetic flux observer. However, in the practical engineering, electromagnetic interference, sensor measurement and error will lead to dc bias in the pure integral link. DC bias will lead to integral saturation in the integral process of pure integral link, which will lead to system instability.

In terms of the current research situation, scholars tend to ignore the existence of iron consumption. However, the iron consumption of induction motor is actual existence. In addition, scholars usually use a first-order low-pass filter instead of a pure integral link to eliminate the cumulative influence of dc bias, but the low-pass filter will produce amplitude and phase errors of flux observation.

The following is a simple example to illustrate the problem. For example:

$$y^* = \int 10 sin(\frac{2\pi}{T} t) dt \tag{4}$$

Add 4% DC bias to the current integral link:

$$y^1 = \int (10 sin(\frac{2\pi}{T} t) + 0.4) dt \tag{5}$$

The function with DC bias is added with a low-pass filter of first order:

$$10\sin(2\pi t/T) + 0.4 \rightarrow 1/(s+\omega_e) \rightarrow y^2 \tag{6}$$

The ω_c=0.7 is cut-off frequency. The low-pass filter is added according to the open-loop voltage model. as shown in the following figure:

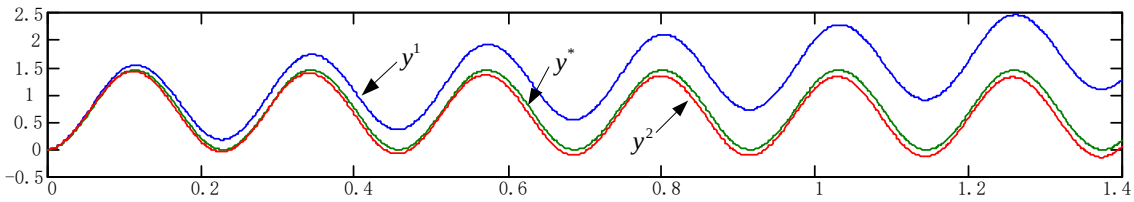

Figure 2. A Low-Pass Filter to example waveform

As we can see from figure 2, using pure integral link, when add 4% of the dc bias, saturation phenomenon appears in the waveform. After adding a first-order low-pass filter, the waveform eliminates the integral saturation phenomenon but in phase and amplitude compared with the original waveform there are still some errors. Therefore, it is necessary to making appropriate compensation for the phase and amplitude.

To solve this problem, this paper adopts the low-pass series high-pass filtering method and compensates the amplitude and phase of the filtered flux. The specific realization principle block diagram is shown in the figure below:

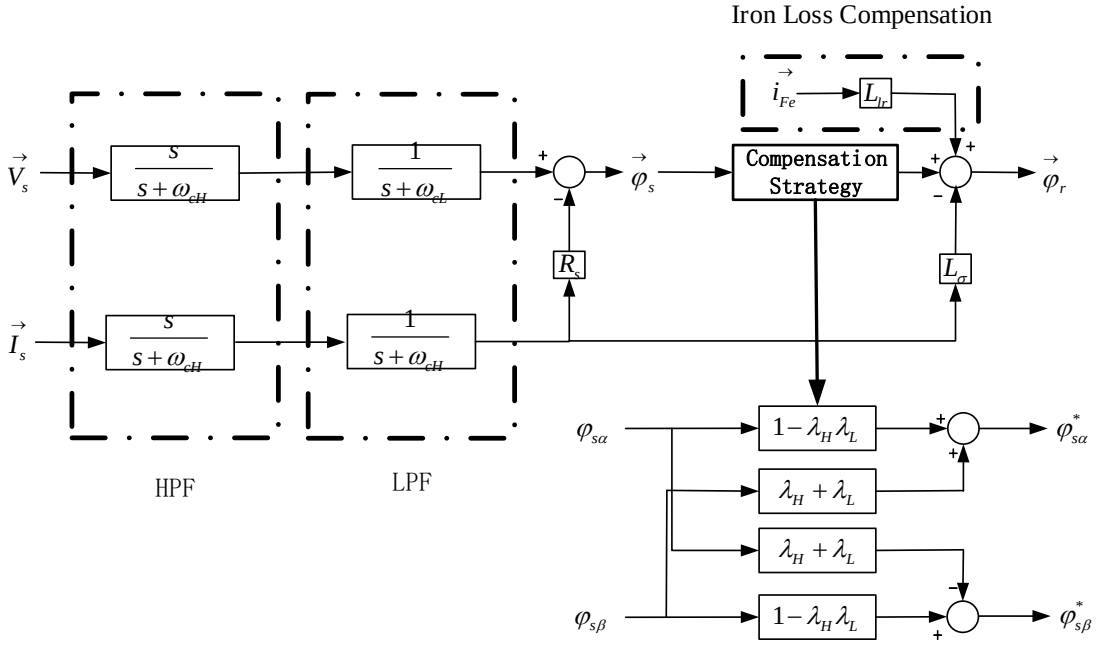

Figure 3. Consider the iron loss of flux observation principle block diagram

The compensation strategy shown in the figure are for the amplitude and phase errors caused by the low-pass and high-pass filters.

Passing through the low-pass filter, the obtained flux is advanced of the actual flux in phase.

$$\varphi_L = -\arctan(\omega_e / \omega_{cL}) \tag{7}$$

According to the above formula, the angle needing to compensate is $-(90-\varphi_L)°$.

However, the error is φ_H in phase to high pass filter.

$$\phi_H = \arctan(\omega_{cH} / \omega_e) \tag{8}$$

Therefore, the angle needing to compensate is $-\varphi_H$.

Meanwhile, comparing with the actual flux in amplitude, we can get the relation as follow:

$$\begin{cases} \left|\vec{V}_s - R_s \vec{I}_s\right| = \left|\vec{\varphi}_L^*\right| \left|j\omega_e\right| \\ \left|\vec{V}_s - R_s \vec{I}_s\right| = \left|\vec{\varphi}_L\right| \left|j\omega_e + \omega_{cL}\right| \end{cases} \tag{9}$$

It's obvious that the parameter of amplitude compensation is as follow:

$$M_L = \sqrt{(\omega_e^2 + \omega_{cL}^2)} / \left|\omega_e\right| \tag{10}$$

Being similar to low pass filter, the compensation of high pass filter is as follow:

$$\left|\vec{\varphi}_s^*\right| = \left|\vec{\varphi}_L\right| \frac{\left|j\omega_e\right|}{\left|j\omega_e + \omega_{cH}\right|} \tag{11}$$

$$M_H = \sqrt{(\omega_e^2 + \omega_{cH}^2)} / \left|\omega_e\right| \tag{12}$$

In conclusion, the total phase compensation is $-(90+\varphi_H-\varphi_L)°$. Meanwhile, the total amplitude compensation is $\sqrt{(\omega_e^2+\omega_{cH}^2)}\sqrt{(\omega_e^2+\omega_{cL}^2)}/|\omega_e|^2$.

We can obtain the following derivation formula to phase compensation as follow:

$$\begin{aligned} e^{-j(90+\varphi_H-\varphi_L)} &= \cos(90+\varphi_H-\varphi_L)-\mathrm{j}\sin(90+\varphi_H-\varphi_L) \\ &= \frac{1}{\sqrt{(\omega_e^2+\omega_{cL}^2)(\omega_e^2+\omega_{cH}^2)}}[(\omega_e^2-\omega_{cL}\omega_{cH})-\mathrm{j}(\omega_e\omega_{cL}+\omega_e\omega_{cH})] \end{aligned} \tag{13}$$

Combined with amplitude compensation, it can be easily obtained that the total compensation to flux observer is as follow:

$$C=[\frac{(\omega_e^2-\omega_{cL}\omega_{cH})}{\omega_e^2}-\mathrm{j}\frac{(\omega_{cL}+\omega_{cH})}{\omega_e}] \tag{14}$$

Furthermore:

$$\begin{aligned} \varphi_{s\alpha}^*+j\varphi_{s\beta}^* &= [\frac{(\omega_e^2-\omega_{cL}\omega_{cH})}{\omega_e^2}-\mathrm{j}\frac{(\omega_{cL}+\omega_{cH})}{\omega_e}](\varphi_{s\alpha}+j\varphi_{s\beta}) \\ &= [\varphi_{s\alpha}\frac{(\omega_e^2-\omega_{cL}\omega_{cH})}{\omega_e^2}+\varphi_{s\beta}\frac{(\omega_{cL}+\omega_{cH})}{\omega_e}]+\mathrm{j}[\varphi_{s\beta}\frac{(\omega_e^2-\omega_{cL}\omega_{cH})}{\omega_e^2}-\varphi_{s\alpha}\frac{(\omega_{cL}+\omega_{cH})}{\omega_e}] \end{aligned} \tag{15}$$

In order to ensure good filtering effect, the paper selects cut-off frequency which is synchronous to frequency's change. That is to say $\omega_{cL}=\lambda_L\omega_e$, $\omega_{cH}=\lambda_H\omega_e$.

By simplifying the above equation (15), the corresponding compensation formula can be obtained as follow:

$$\varphi_{s\alpha}^*+j\varphi_{s\beta}^*=[\varphi_{s\alpha}(1-\lambda_L\lambda_H)+\varphi_{s\beta}(\lambda_L+\lambda_H)]+\mathrm{j}[\varphi_{s\beta}(1-\lambda_L\lambda_H)-\varphi_{s\alpha}(\lambda_L+\lambda_H)] \tag{16}$$

In normal conditions, $\lambda_L=2\lambda_H$. According to the literature [6-7], we can know the best value of λ_L is 0.2~0.3. Meanwhile, the lower limiting value is 1 rads/s, which is to avoid larger timer constant when the motor's speed is in lower velocity values.

3. Simulation

The parameters of asynchronous motor are shown in the table:

Table 1. Motor parameters

V_{rated}：1287V	Rs：0.223Ω
I_{rated}：88A	Rr：0.103Ω
P_{rated}：160KW	L_m：43.8mH
n_{rated}：2520rpm	L_{ls}：1.58mH
n_{peak}：4723rpm	L_{lr}：2.076mH
f_{rated}：84Hz	p：2
η_{rated}：93%	T_{emax}：1335N.m
$Flux_{rated}$：1.4Wb	cosΦ：0.86

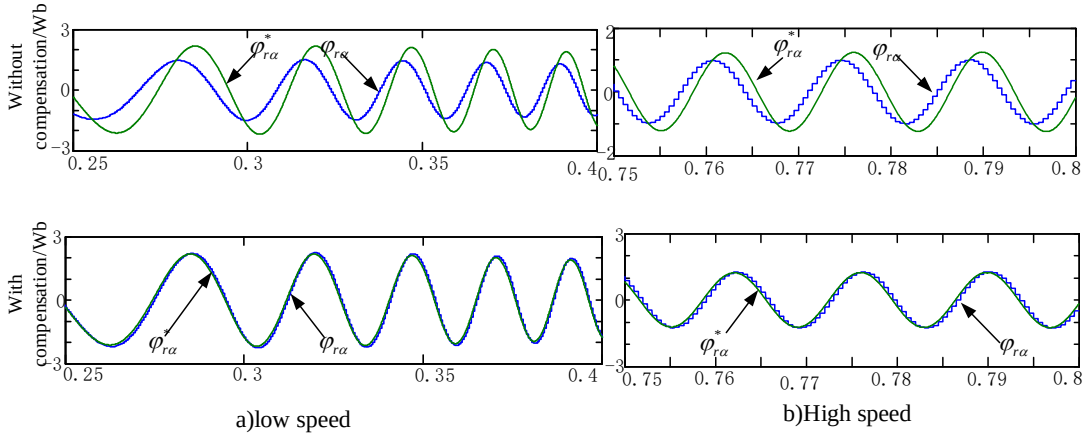

Figure 4. The differences between the HPF+LPF with compensation and without compensation

As shown in the figure above, the asynchronous motor runs in the low-speed section and the high-speed section respectively. In the high-speed section, the motor has entered the weak magnetic condition. Considering the waveform of the compensated and uncompensated flux linkage, it is obvious that the phase and amplitude of the flux linkage are greatly deviated without compensation. After the addition of phase and amplitude compensation, the observed flux of the motor can accurately track the actual flux value of the motor no matter in the link of low speed or high speed of the motor.

In order to further verify the accuracy and stability of flux observation of the voltage model considering iron consumption after improvement, simulation software is used to record the flux observation effect when the motor speed changed from 600rpm to 2100rpm.

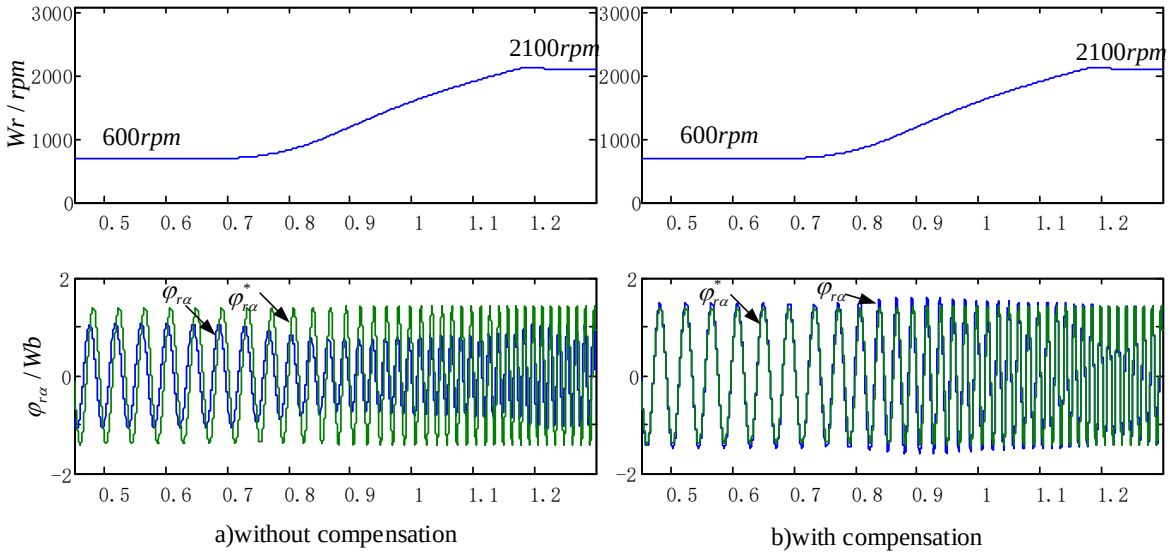

Figure 5. The comparison between the HPF+LPF with compensation and without compensation when motor's speed is up

In the figure above, the left side is the comparison of magnetic flux observation waveform of the motor in the process of lifting speed from 600rpm to 2100rpm without adding amplitude and phase compensation. Meanwhile the right side is the comparison of magnetic flux observation waveform of the motor in the process of lifting speed from 600rpm to 2100rpm without adding phase and phase compensation. It can be seen from the figure that in the process of motor's speed growing, the

improved voltage model observation considering iron loss can accurately observe the motor flux. In addition, the phenomenon of non-integral saturation appears.

4. Experiment

In order to further verify the method proposed in this paper, DSP+FPGA programming and virtual instrument monitoring are adopted based on the test platform composed of actual induction motor and two-level IGBT inverter. The dc voltage used in the experiment is 1650V, and the motor parameters are the same as mentioned in the simulation. In this test, DA is used to display the actual speed and rotor flux of the motor.

Figure 6. The motor for testing system and the equipment to save waveform

As shown in the figure below for asynchronous motor at full speed range, the motor's frequency is 5 Hz、20 Hz、70 Hz and 120 Hz. It's obvious that the optimized flux observer mentioned in this paper is normal and its feature of sine is preferably. What's more, the track of rotor flux is round which is no integral saturation phenomenon and no drift phenomena happen. Moreover, when the motor speed reaches 120Hz, the motor is already in a weak magnetic region. At this frequency, it can be seen from the figure that the track area of the rotor flux is significantly smaller than that of the constant excitation region. In this region, the flux observation still has good stability performance.

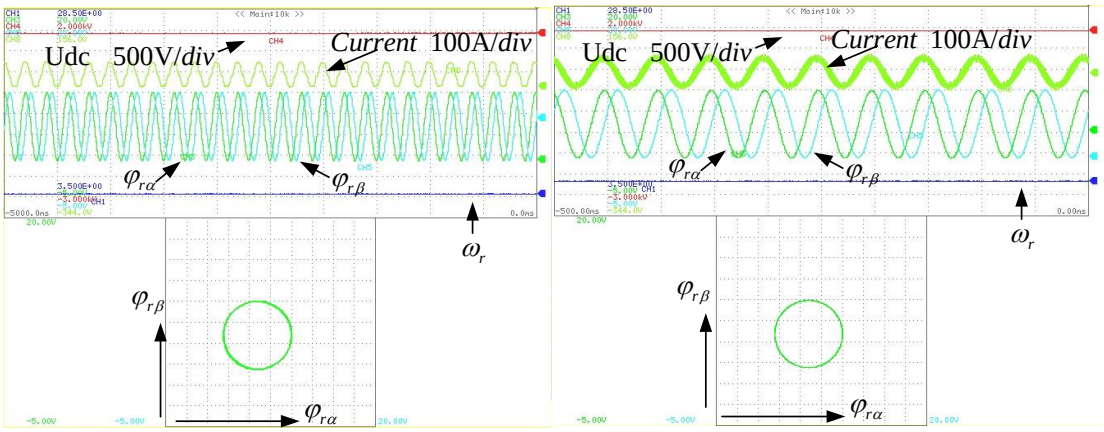

a)5Hz b)20Hz

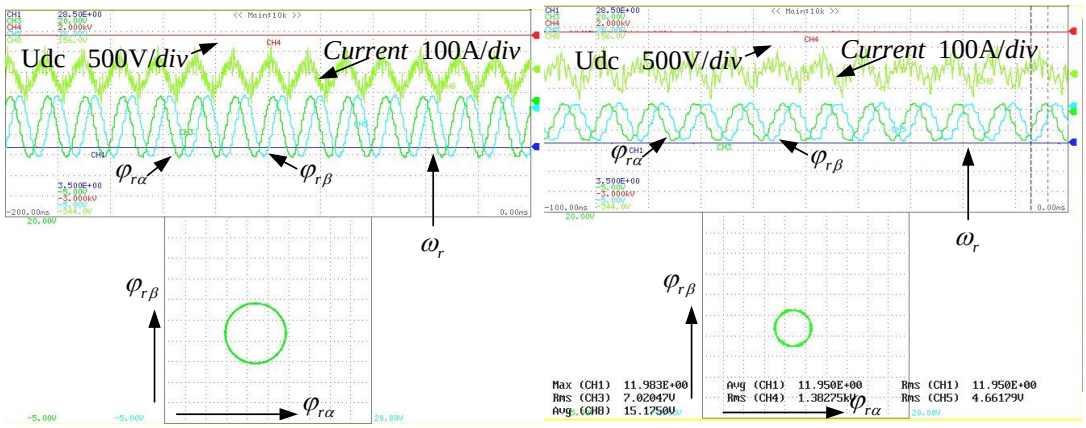

c)70Hz d)120Hz

Figure 7. Flux estimation of motor in full speed range

In the process of test, we find that there is a problem worthy of attention which when the motor under the magnetic field of negative reverse rotation, due to the synchronous angular frequency of the motor and motor speed are negative, low-pass and high-pass filter transfer function is positive pole. In consequence, the system is divergent. Therefore, the two cut-off frequency must remain positive.

The left side of the figure shows that the zero point treatment is not considered. It is obvious that the system become divergent from stable. However,when the zero crossing point is processed, the motor can still ensure the stable observation of the magnetic linkage even when it is reversed.

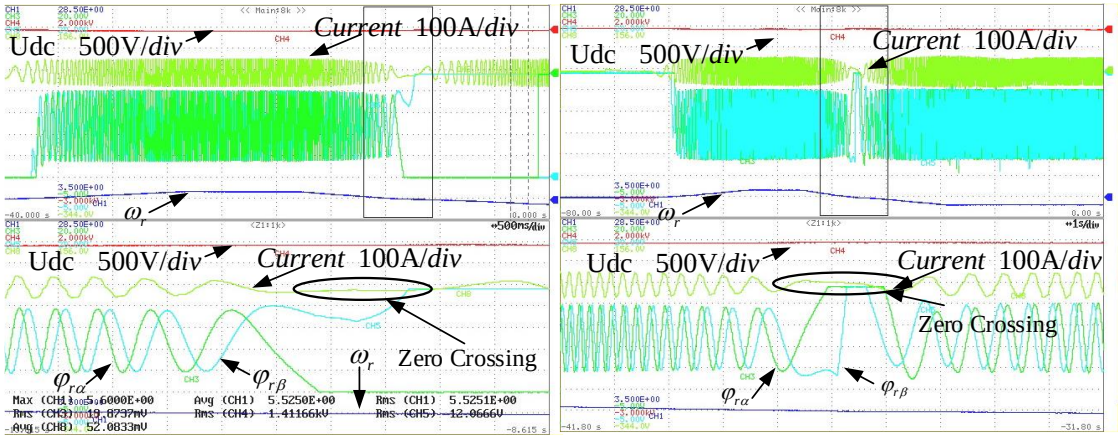

Figure 8. Comparison of flux observation between with and without conducting in zero point

In conclusion, the improved voltage-model flux observer method considering iron consumption mentioned in this paper can accurately observe the flux on the rotor side of the motor, and obtain better dynamic and problem performance within the full speed range.

5. Conclusion

In this paper, the improved voltage-model flux observer method considering iron consumption mentioned in this paper can accurately observe the flux on the rotor side of the motor, and obtain better dynamic and problem performance within the full speed range. The feasibility and validity of the theory in this paper are verified through simulation and experiment.

References

[1] BOSE B K. (2005) Modern Power Electronics and AC Drives. Machine Press, Beijing China.

[2] B. Kou, L. Li, S. Cheng, and F.Meng.(2005) Operating Control of Efficiently Generating Induction Motor for Driving Hybrid Electric Vehicle. IEEE Transactions on Magnetics, Vol.41, No.1, January.
[3] Ho Shin Myoung, Seok Hyun Dong. (2008) An improved staor flux estimation for speed sensorless stator flux orientation control of induction motors. PESC, 15(2):1581-1586.
[4] Seyoum D G, Rahman C. (2003).Simplified flux estimation for control application in induction machines.IEMDC,3(2):691-695.
[5] Hu Hu, Yong Dong Li. (2002) Direct torque control of induction motor for railway traction in whole speed range. IECON,2(6):2161-2166.
[6] Nik Rumzi Nik Idris, Abdul Halim Mohamed Yatim. (2000) An improved stator flux estimation in steady-state operation for direct torque control of inductor machines. Industry Applications, IEEE Transactions, 38(3):110-116.
[7] ZHANG Xu, QU Wenlong. (2003) A novel compensation method of stator flux estimating in low speed region. Advanced Technology of Electrical Engineering and Energy, ,22(2):50-53.